

Room temperature 2D electron gas at the (001)-SrTiO_3 surface

Sara Gonzalez, Claire Mathieu, O. Copie, Vitaliy Feyer, Claus M Schneider, Nicholas Barrett

▶ **To cite this version:**

Sara Gonzalez, Claire Mathieu, O. Copie, Vitaliy Feyer, Claus M Schneider, et al.. Room temperature 2D electron gas at the (001)-SrTiO_3 surface. Applied Physics Letters, 2017, 111, pp.181601. 10.1063/1.5001222 . cea-01704463

HAL Id: cea-01704463
https://cea.hal.science/cea-01704463

Submitted on 8 Feb 2018

HAL is a multi-disciplinary open access archive for the deposit and dissemination of scientific research documents, whether they are published or not. The documents may come from teaching and research institutions in France or abroad, or from public or private research centers.

L'archive ouverte pluridisciplinaire **HAL**, est destinée au dépôt et à la diffusion de documents scientifiques de niveau recherche, publiés ou non, émanant des établissements d'enseignement et de recherche français ou étrangers, des laboratoires publics ou privés.

Room temperature 2D electron gas at the (001)-$SrTiO_3$ surface

Sara Gonzalez,[1] Claire Mathieu,[1] Olivier Copie,[1,2] Vitaliy Feyer,[3,4] Claus M. Schneider,[4,5] and Nicholas Barrett[1,a)]

[1]*SPEC, CEA, CNRS, Université Paris Saclay, F-91191 Gif-sur-Yvette, France*
[2]*Institut Jean Lamour, UMR 7198 CNRS/Université de Lorraine, 54056 Vandoeuvre-lès-Nancy, France*
[3]*NanoESCA Beamline, Sincrotrone Trieste, Area Science Park, 34149 Basovizza, Trieste, Italy*
[4]*Peter Grünberg Institute (PGI-6), JARA-FIT, Research Center Jülich, 52425 Jülich, Germany*
[5]*Fakultat f. Physik and Center for Nanointegration Duisburg-Essen (CENIDE), Universität Duisburg-Essen, D-47048 Duisburg, Germany*

(Received 23 August 2017; accepted 13 October 2017; published online 31 October 2017)

Functional oxides and phenomena such as a 2D electron gas (2DEG) at oxide interfaces represent potential technological breakthroughs for post-CMOS electronics. Non-invasive techniques are required to study the surface chemistry and electronic structure, underlying their often unique electrical properties. The sensitivity of photoemission electron microscopy to chemistry and electronic structure makes it an invaluable tool for probing the near surface region of microscopic regions and domains of functional materials. We present results demonstrating a room temperature 2DEG at the (001)-$SrTiO_3$ surface. The 2DEG is switched on by soft X-ray irradiation. *Published by AIP Publishing.*
https://doi.org/10.1063/1.5001222

$SrTiO_3$ (STO) is the preferred template to create a two-dimensional electron gas (2DEG), thus forming a potential basis for oxide electronics as an alternative to silicon technologies.[1,2] 2D conducting states were initially observed at the interface between STO and another band insulator, $LaAlO_3$, (Ref. 3) and have since also been unveiled at the surface of a bare STO single crystal.[4–6] A variety of mechanisms have been invoked to explain the formation and behavior of 2D metallic states at the STO surface, including oxygen pumping via Al capping,[7] defect states,[4,8] reduction under ultraviolet radiation,[9,10] and field-induced gating.[11]

The electronic structure can be assessed by photoelectron emission techniques and in particular angle-resolved photoelectron spectroscopy (ARPES). The highest spectroscopic resolution, allowing one to resolve 2D and 3D band characters, calculate the Fermi surface (FS) volume, and estimate the electron effective mass, is obtained at low temperature, typically 10–20 K.[9,12] Nevertheless, any realistic oxide based electronics must obviously work at room temperature (RT). Therefore, the study of the 2DEG band structure at the surface of STO at RT has to be conducted. RT scanning tunneling spectroscopy has demonstrated 2D electron confinement following moderate annealing in vacuum.[6] The existence of a low binding energy (BE) shoulder in the Ti 2p core level spectrum due to reduced Ti is a necessary condition for a 2DEG in STO; however, by itself it is not sufficient since the Ti^{3+} shoulder may also be due to localized electrons which cannot contribute to the quasiparticle at the Fermi level (FL).[10]

Here, we use photoemission electron microscopy (PEEM) and synchrotron radiation to characterize the Fermi surface (FS) of STO and to directly observe the existence of a 2DEG at room temperature, showing clearly the band structure of a highly mobile 2DEG, which can be obtained with a simple surface STO surface preparation. PEEM has the advantage of rapid switching between real and reciprocal space imaging, allowing correlation of surface chemistry with the electronic band structure on a microscopic scale.[13,14] The field of view (FoV) is a few microns, much smaller than typical beam spots in an ARPES experiment at a synchrotron source. Thus, band structure analysis by PEEM also allows selecting a high quality, homogeneous area of the surface. Reciprocal space PEEM, or k-PEEM, acquires constant energy cuts $I(k_x, k_y)$, thus allowing one shot Fermi surface acquisition. In this way, the FS can be directly monitored, for example, as a function of redox conditions or during reduction under intense UV irradiation.

A 0.5% Nb-doped, TiO_2-terminated, STO (supplied by SurfaceNet GmbH) was cleaned by a 5 min ozone treatment before insertion into ultrahigh vacuum, where it was annealed at 873 K for 2 h at a base pressure of 4×10^{-7} Pa. After annealing, we checked the STO surface order using low-energy electron diffraction (LEED). The sharp, (1×1) LEED pattern shows a (1×1) surface reconstruction attesting to the high surface structural quality [Fig. 1(a)].

The experiments were performed with a NanoESCA photoemission spectrometer at the Elettra synchrotron.[13] The base pressure was better than 2×10^{-8} Pa. The band structure of the STO was measured at 300 K using the reciprocal space imaging mode of the NanoESCA with an energy resolution of 0.2 eV. In the reciprocal space imaging mode or k-PEEM, the photoelectrons are detected with a wave vector resolution of about 0.05 $Å^{-1}$ for all $k_{\|}$. The Fermi level (FL) region was recorded for photon energies between 30 and 100 eV in 2 eV steps. High resolution image series were taken at 47.8 and 82 eV, corresponding to a point close to the Brillouin zone edge and to Γ_{003}, using both horizontal and vertical polarizations. The image series were taken over 0.8 eV around the FL in 0.019 eV steps. As shown in Figs. 4(a)–4(d), at the FS around the Γ_{00} point, three Brillouin zones are recorded in a single image. Sr 3d and Ti 2p core level spectra were acquired with higher photon energy, 654.4 eV and the same energy resolution.

a)Author to whom correspondence should be addressed: nick.barrett@cea.fr

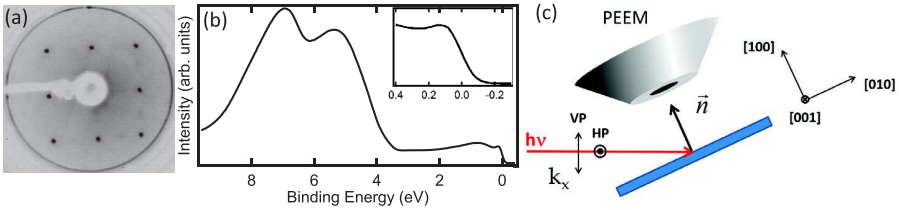


FIG. 1. (a) (1 × 1) LEED (electron energy 66 eV). (b) Valence band spectrum taken at $h\nu = 82.11$ eV showing gap states and metallic 2DEG at FL. (c) Geometry used for these k-PEEM experiments.

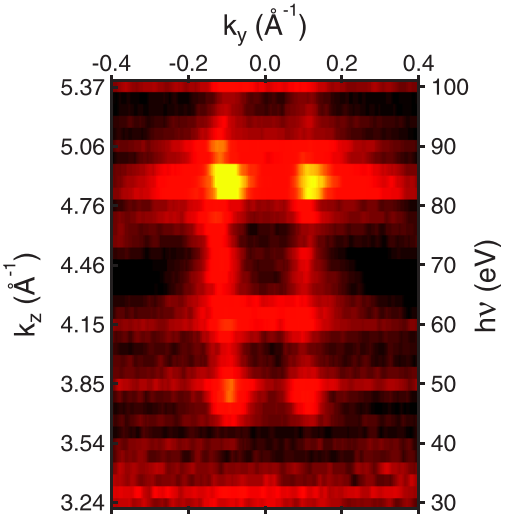


FIG. 2. k_y-k_z map of the 2D state, located at $k_x = 0$ Å^{-1}. The corresponding photon energy is also presented. Photon energy 30 to 100 eV with an inner potential of 14.5 eV (Ref. 15) and a WF of 4.5 eV gives $k_z = 3.24$ to 5.37 Å^{-1}.

Figure 1(b) shows the valence band spectrum obtained from a 10 μm FoV, with a photon energy of 82.11 eV, calibrated using the Fermi level. The main structure due to the O 2p states dominates the spectrum between 4 and 8 eV binding energy (BE). The valence band maximum is at ~3.4 eV. Assuming a bandgap of 3.2 eV, this is consistent with the surface state bandwidth of 0.2 eV, reported below. Intensity due to states resulting from oxygen vacancies is present in the gap at ~1 eV below the FL. As can be seen in the inset, a sharp Fermi edge is visible, due to the 2DEG.

We have recorded a constant energy cut at ~0.08 eV below the FL for photon energies between 30 and 100 eV corresponding to k_z between 3.24 and 5.37 Å^{-1}, respectively, assuming an inner potential of 14.5 eV and the measured work function value of 4.5 eV. The results are shown as a k_y-k_z plot in Fig. 2. The non-monotonic intensity variations with photon energy are probably mainly due to variations in the matrix elements.[4,16] As can be seen, there is no dispersion of the state with k_z, proving its 2D nature.

The Ti 2p and Sr 3d core level spectra, recorded at a photon energy of 654.4 eV, are shown in Fig. 3. The Ti $2p_{3/2}$ shows a main peak at a BE of 459.1 eV, corresponding to Ti^{4+},[17] and a clear shoulder at 2.0 eV lower binding energy, due to Ti^{3+}.[15,18] Two more components, at higher binding energy, are required to fit the Ti 2p spectrum, associated with satellite peaks due to intrinsic loss processes.[17,19] The Ti^{3+} component is a clear signature of a reduced surface, consistent with the formation of a metallic-like Fermi edge. We find a larger full width at half maximum (FWHM) for the Ti^{3+} component (1.77 eV) than for the dominant doublet (1.11 eV).[17]

Figure 3 also shows the Sr 3d doublet and the best least squares fit using two components. The main component at 133.7 eV for the $3d_{5/2}$ is due to the Sr in the bulk STO. The weaker, high binding energy (HBE) component is shifted by 1.0 eV and represents Sr in the near surface environment. The FWHM for both doublets is the same, indicating that the core hole lifetime should be the same near the surface and in the bulk. The HBE peak may be due to the formation of SrO[20] at the surface under UV irradiation[10] but also to an electrostatic modification or band bending at the surface,[15,17] linked to the formation of the 2D metallic surface state.

Figure 4 shows the single shot FS images taken at $h\nu = 47.8$ eV and 82.0 eV, using horizontally (HP) and vertically (VP) polarized light [s and p polarization with respect to the plane of incidence, see schematic Fig. 1(c)]. The STO (100) work function was 4.5 eV. Assuming an inner potential of 14.5 eV, these energies correspond to $k_z = 3.9$ and 4.9 Å^{-1},[15] i.e., on the edge and at the center of the Brillouin zone.

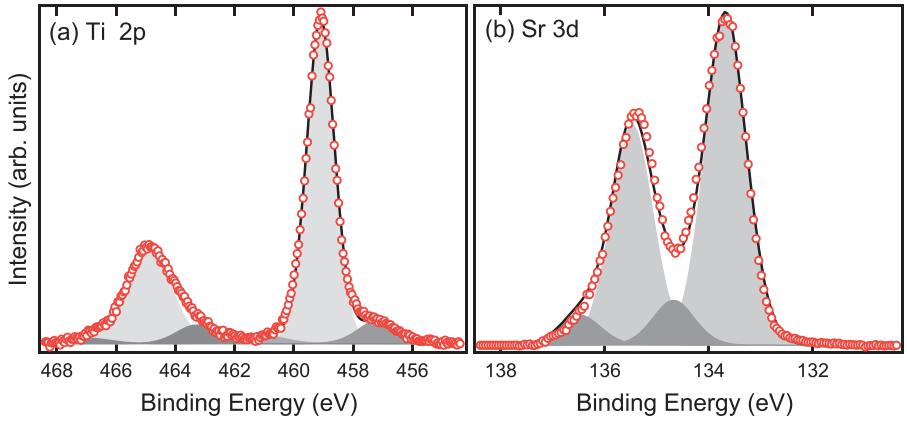


FIG. 3. (a) Ti 2p core level with low binding energy shoulder due to beam-induced Ti^{3+}. (b) Sr 3d core level showing strong asymmetry to high binding energy (HBE). The HBE peak is due to the proximity of the 2D metallic surface. The spectra have been recorded with a photon energy of 654.4 eV.

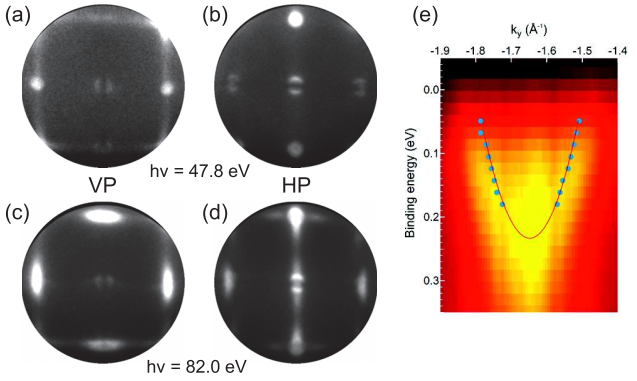


FIG. 4. (a)–(d) Fermi surfaces acquired at room temperature for both vertical and horizontal light polarization at $h\nu = 47.8$ (a) and (b) and 81.9 eV (c) and (d) ($k_z = 3.9$ and 4.9 Å^{-1}, respectively, at the edge and at the center of the Brillouin zone, $2\pi/a = 1.61$ Å^{-1}). (e) k_y-E cut at $k_x = 0$ showing the momentum distribution curves and the dispersion of the 2DEG $3d_{xy}$. The parabolic fit (red line) to the lowest d_{xy} subband and the maxima used to perform the fit (blue dots) are superimposed on the figure.

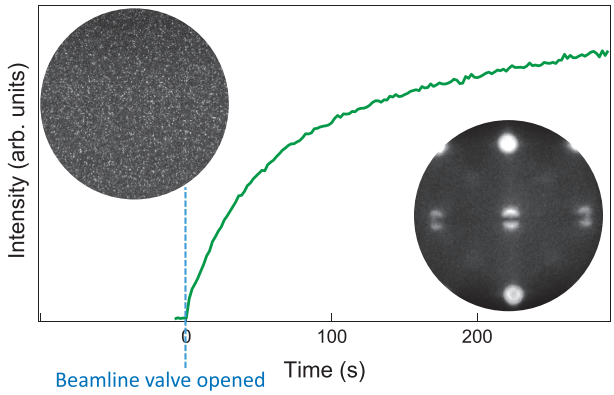


FIG. 5. Intensity of the k-space image recorded ~0.08 eV below the Fermi level, as a function of the exposure time to the synchrotron beam. The k-space images recorded before and after exposure to beam are shown in the upper right and bottom left of the figure, respectively.

The FSs agree well in shape and size with those observed at low temperature, see, for example, Refs. 4 and 15. At 82.0 eV, the heavier Ti $3d_{xz/yz}$ states are visible using VP (p) light, whereas the light Ti $3d_{xy}$ states are revealed by the HP light (s polarization). The lighter 2D surface states are observed for both VP and HP light. The only difference with respect to the low temperature ARPES data is the sharpness of the FS structures. This is due to the experimental resolution (0.2 eV) and the fact that the measurements were carried out at room temperature, for which 4 kT ~100 meV.

The waterfall image of Fig. 4(e) shows a k_y -E dispersion at $k_x = 0$ of the 2DEG state acquired in HP at $h\nu = 82.0$ eV. The dispersion is fitted by a free electron-like parabola corresponding, within the experimental resolution, to the first d_{xy} subband. From the fit, the effective mass can be estimated as $0.2m_e$, in agreement with the values obtained by Santander-Syro[4] and McKeown-Walker.[9] The 2D carrier density, defined by $n_{2D} = k_F^2/2\pi$, can be obtained by measuring the Fermi momenta (k_F). The measured $k_F = 0.169$ Å^{-1} leads to a 2D carrier density of 4.57×10^{13} cm^{-2}, consistent with the literature values at low temperature.[4,15] As mentioned in the introduction, the 2DEG at the surface of STO may be created by a variety of mechanisms. Indeed, the annealing is expected to play a role in the 2DEG creation. However, it appears here to be due to beam interaction with the surface, reducing Ti^{4+} to Ti^{3+} and creating a 2D metallic surface state. This was confirmed by a second series of k-PEEM experiments (this time performed at 140 K in order to improve the resolution). For these measurements, once the PEEM settings were optimized, the sample was moved so as to expose a fresh surface region to the synchrotron beam at 82 eV.

FS images were then acquired as a function of exposure time to the beam. Figure 5 shows the time evolution of the angle-integrated intensity of the FS under beam. Initially, there is zero intensity at the FL which implies that annealing alone during surface preparation does not create a 2DEG. After 4 min exposure to the beam, a sharp FS is obtained, identical to that observed at room temperature in Fig. 4. The longer the surface is exposed to the beam, the more intense the features are. For even longer exposure times, the intensity appears to approach a saturation value. This shows that the beam exposure has a greater effect on the creation of the 2DEG than the annealing used to prepare the surface and that the 2DEG is populated by electrons freed following the creation of oxygen vacancies at the surface.[9,10]

Spectra of the Ti 2p core-level (not shown) exhibited a higher Ti^{3+} component after the beam exposure, reinforcing the fact that the beam is responsible for reduced Ti^{4+} rather than the annealing.[10] This sensitivity of the 2DEG to the oxygen partial pressure may limit the possibilities of realistic electronic devices to oxide structures with buried interfaces such as LAO/STO.

In conclusion, we have used PEEM to observe the formation of a 2DEG at room temperature at the surface of STO(100). The STO surface was prepared by *ex-situ* ozone exposure followed *in-situ* by simple UHV annealing at 873 K for 2 h. The Fermi surface appears as a result of reduction under intense UV light and is identical to that widely observed at low temperature.

This work was supported by the Triangle de la Physique ELOXIR project. We acknowledge Sincrotrone Elettra for the provision of synchrotron radiation facilities.

[1]C. Cen, S. Thiel, J. Mannhart, and J. Levy, Science **323**, 1026 (2009).
[2]M. Bibes, J. E. Villegas, and A. Barthélémy, Adv. Phys. **60**, 5 (2011).
[3]A. Ohtomo and H. Y. Hwang, Nature **427**, 423 (2004).
[4]A. F. Santander-Syro, O. Copie, T. Kondo, F. Fortuna, S. Pailhès, R. Weht, X. G. Qiu, F. Bertran, A. Nicolaou, A. Taleb-Ibrahimi, P. Le Fèvre, G. Herranz, M. Bibes, N. Reyren, Y. Apertet, P. Lecoeur, A. Barthélémy, and M. J. Rozenberg, Nature **469**, 189 (2011).
[5]W. Meevasana, P. D. C. King, R. H. He, S.-K. Mo, M. Hashimoto, A. Tamai, P. Songsiriritthigul, F. Baumberger, and Z.-X. Shen, Nat. Mater. **10**, 114 (2011).
[6]R. Di Capua, M. Radovic, G. M. De Luca, I. Maggio-Aprile, F. Miletto Granozio, N. C. Plumb, Z. Ristic, U. Scotti di Uccio, R. Vaglio, and M. Salluzzo, Phys. Rev. B **86**, 155425 (2012).
[7]T. C. Roedel, F. Fortuna, S. Sengupta, E. Frantzeskakis, P. Le Fèvre, F. Bertran, B. Mercey, S. Matzen, G. Agnus, T. Maroutian, P. Lecoeur, and A. F. Santander-Syro, Adv. Mater. **28**, 1976 (2016).
[8]L. Dudy, M. Sing, P. Scheiderer, J. D. Denlinger, P. Schuetz, J. Gabel, M. Buchwald, C. Schlueter, T. L. Lee, and R. Claessen, Adv. Mater. **28**, 7443 (2016).
[9]S. McKeown Walker, F. Y. Bruno, Z. Wang, A. de la Torre, S. Ricco, A. Tamai, T. K. Kim, M. Hoesch, M. Shi, M. S. Bahramy, P. D. C. King, and F. Baumberger, Adv. Mater. **27**, 3894 (2015).

[10]J. Gabel, M. Zapf, P. Scheiderer, P. Schuetz, L. Dudy, M. Stuebinger, C. Schlueter, T.-L. Lee, M. Sing, and R. Claessen, Phys. Rev. B **95**, 195109 (2017).
[11]H. Nakamura, T. Koga, and T. Kimura, Phys. Rev. Lett. **108**, 206601 (2012).
[12]S. McKeown Walker, S. Ricco, F. Y. Bruno, A. De La Torre, A. Tamai, E. Golias, A. Varykhalov, D. Marchenko, M. Hoesch, M. S. Bahramy, P. D. King, J. Sánchez-Barriga, and F. Baumberger, Phys. Rev. B: Condens. Matter Mater. Phys. **93**, 245143 (2016).
[13]C. Schneider, C. Wiemann, M. Patt, V. Feyer, L. Plucinski, I. Krug, M. Escher, N. Weber, M. Merkel, O. Renault, and N. Barrett, J. Electron Spectrosc. Relat. Phenom. **185**, 330 (2012).
[14]J. E. Rault, J. Dionot, C. Mathieu, V. Feyer, C. M. Schneider, G. Geneste, and N. Barrett, Phys. Rev. Lett. **111**, 127602 (2013).
[15]N. C. Plumb, M. Salluzzo, E. Razzoli, M. Månsson, M. Falub, J. Krempasky, C. E. Matt, J. Chang, M. Schulte, J. Braun, H. Ebert, J. Minár, B. Delley, K. J. Zhou, T. Schmitt, M. Shi, J. Mesot, L. Patthey, and M. Radović, Phys. Rev. Lett. **113**, 086801 (2014).
[16]S. G. Louie, P. Thiry, R. Pinchaux, Y. Petroff, D. Chandesris, and J. Lecante, Phys. Rev. Lett. **44**, 549 (1980).
[17]G. M. Vanacore, L. F. Zagonel, and N. Barrett, Surf. Sci. **604**, 1674 (2010).
[18]A. E. Bocquet, T. Mizokawa, K. Morikawa, A. Fujimori, S. R. Barman, K. Maiti, D. D. Sarma, Y. Tokura, and M. Onoda, Phys. Rev. B **53**, 1161 (1996).
[19]M. Oku, H. Matsuta, K. Wagatsuma, Y. Waseda, and S. Kohiki, J. Electron Spectrosc. Relat. Phenom. **105**, 211 (1999).
[20]S. A. Chambers, T. C. Droubay, C. Capan, and G. Y. Sun, Surf. Sci. **606**, 554 (2012).